was acquired at t = 0, 2, 4, 6, 8, and 10 minutes. Treatment and MR scanning was performed on voided bladders. The bladder CTV was delineated in all scans and each CTV was described using spherical coordinates with origin at the centre of volume of the first scan of the first session of each patient. Population-based 2D margin maps were derived by adapting a published margin recipe for bladder (Meijer et al, IJROBP 2003), characterising in the spherical coordinate system the intra-fractional changes (between the scans at t = 0 min to t = 10 min) in terms of systematic and random errors. Secondly, the possibility of deriving patient-specific intra-fractional margins was explored by using only the bladder expansions occurring in the first two series (the pre-treatment and the first week series). A linear model was used to fit the radial changes occurring as a function of time. Focusing on the patients and directions where an expansion larger than 5 mm was observed, the patient-specific margin was defined as the upper 96% confidence limit of the linear coefficient multiplied by the relevant intra-fractional time (here assumed ten minutes).

Results: The population-based 2D margin map is shown in Fig 1; when excluding the one female patient, the margins at superior and anterior directions were 14 mm, posterior 9 mm and the other directions (inferior, left and right) 5 mm. Intra-fractional margins specific for each patient could be derived from the linear model fit (ranging up to 12 mm; R2 in the range: 0.33-0.68).

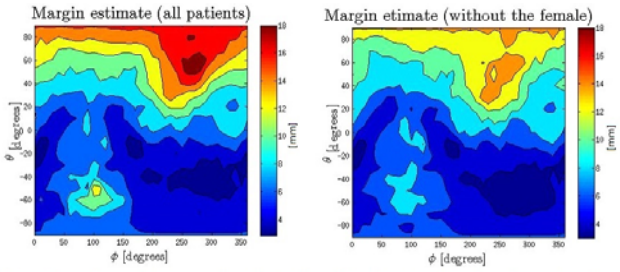

Figure 1: 2D-maps of the population-based margins, showing both the margins for all nine patients (left) and the margins when the one female patient was excluded. Superior direction is found at θ = 90° and inferior at θ = -90°. Anterior, posterior as well as left and right directions are seen for θ = 0°, with posterior at φ = 90°, anterior at φ = 270°, left at φ = 0°/360°, and right at φ = 180°.

Conclusions: This is the first study to present both population-based and patient-specific margins for intra-fractional motion for the bladder. The population-based margins were large in superior and anterior directions, and are a concern in particular if pursing on-line re-planning/optimization.We also found that the large intra-fractional margins required for some patients can be identified and estimated from limited data on bladder expansions from scans acquired before or early in the treatment course.

PD-0462

Towards dosimetric tracking with adaptive VMAT?

W. Crijns[1], G. Defraene[1], H. Van Herck[2], T. Depuydt[1], K. Haustermans[1], F. Maes[3], F. Van den Heuvel[4]

[1]KU Leuven, Department of Oncology Laboratory of Experimental Radiotherapy, Leuven, Belgium

[2]KU Leuven, Medical Imaging Research Center, Leuven, Belgium

[3]KU Leuven, Department of Electrical Engineering (ESAT) - PSI Center for the Processing of Speech & Images, Leuven, Belgium

[4]KU Leuven, Department of Oncology MRC-CR-UK Gray Institute of Radiation Oncology and Biology, Leuven, United Kingdom

Purpose/Objective: Target tracking during RT is taking its first steps in clinical practice. The next challenge is correcting for organ motion induced dosimetric deviations (due to tissue heterogeneity, distance to source variations, etc.). A VMAT adaptation strategy has been developed and was evaluated using 3D dose measurements in a dynamic prostate phantom.

Materials and Methods: An initial VMAT plan ($Plan_0$) was optimized in Eclipse to deliver 77Gy with an integrated focal boost (prostate: 2.2Gy; boost 2.7Gy/fraction) to the prostate of the Dynamic Pelvis Phantom (CIRS, Virginia, USA, Figure 1, upper panel). Different realistic prostate motions[1] were executed by the phantom; and for each, three different VMAT treatment adaptation strategies were measured:
1) The current clinical practice: delivery of $Plan_0$ without plan correction.
2) MLC-only: a correction of the MLC positions of $Plan_0$ according to the tracked target position.
3) A MLC+MU adaptation, which uses point dose calculations to correct MU per gantry angle in addition to the MLC correction.
All corrections were driven by the positions of four fiducial points.
3-D dose of each strategy was measured using a stack of EBT films inserted in the phantom (10 planes [63.50x63.50mm^2] seperated by 4.16mm). Next, DVHs are calculated for the measured dose planes and corresponding calculated planes. VMAT delivery and phantom motions were synchronized to enable comparison of different treatment strategies for a given motion pattern.

Results: Measurements without motion agreed with the intended $Plan_0$. For a prostate drift motion (Figure 1, lower panel), all treatment strategies showed a blurring of the prostate dose (less steep DVHs), and a consequently increased dose to the part of the rectum included in the measurement volume.
Without adaptation, the prostate and boost dose were reduced compared to $Plan_0$ (Clinical practice: $D_{95\%\ Prostate}$= 93%, $D_{95\%\ Boost}$ = 96%), both adaptation strategies improved the target coverage (MLC: $D_{95\%\ Prostate}$= 100%, $D_{95\%\ Boost}$ = 104%; MLC+MU: $D_{95\%\ Prostate}$= 97%, $D_{95\%\ Boost}$ = 100%).
For the boost volume, which is surrounded by less steep dose gradients, no blurring was observed and the MLC+MU adaptation coincided completely with the intended dose, while the lack of MU correction of the MLC-only adaptation showed an increased boost dose.

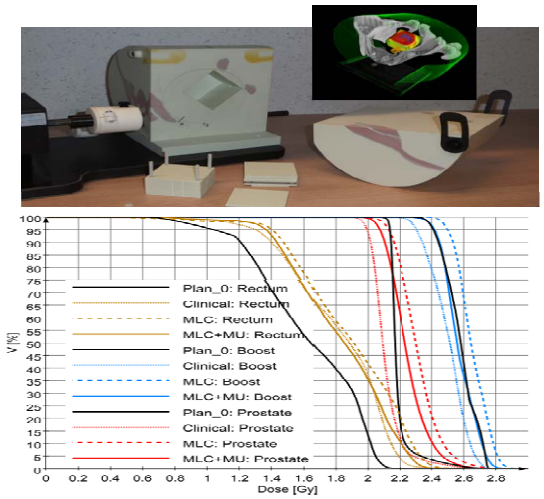

Figure 1 : Upper panel: prostate motion phantom used for 3D dose measurements (inset). Lower panel: DVH comparison of the different treatment strategies for prostate drift motion: clinical practice (dotted-line), MLC

adaptation (dashed-line), and MLC+MU adaptation (full-line). The intended plan ($Plan_0$) is depicted in black.

Conclusions: All treatment strategies showed reduced dose gradients (blurring), decreased target coverage, and increased dose to the rectum inside the measuring volume. Both adaptation strategies improved target coverage compared to the clinical practice, but MLC-only (tracking) results in an overdose for the targets while MLC+MU (dosimetric tracking) rectifies this overdose. These results are confirmed using more complex motion patterns. The applied adaptation strategies can be implemented in real time.

PD-0463

Characterization of target registration error using radiopaque markers implanted in the lung

M. Takamiya[1], M. Nakamura[2], M. Akimoto[2], N. Ueki[2], H. Tanabe[3], Y. Matsuo[2], T. Mizowaki[2], M. Kokubo[4], M. Hiraoka[2], A. Ito[1]

[1]Kyoto University Graduate School of Engineering, Nuclear Engineering, Kyoto, Japan
[2]Kyoto University Graduate School of Medicine, Radiation Oncology and Image-applied Therapy, Kyoto, Japan
[3]Kobe City Medical Center General Hospital, Radiation Oncology, Hyogo, Japan
[4]Institute of Biomedical Research and Innovation, Radiation Oncology, Hyogo, Japan

Purpose/Objective: Recently, respiratory managing techniques, such as respiratory gating and dynamic tumor tracking (DTT), have been widely used in clinical practice. These techniques often need fiducial markers implanted around the target to localize the tumor position. Distance from radiopaque markers to a target (|d|) and difference in range of respiratory motion between the radiopaque markers and the target (ΔRM) were mainly considered as the factors in the target registration error (TRE) for these techniques. The purpose of study was to investigate the impact of |d| and ΔRM on the TRE.

Materials and Methods: This study included 15 lung cancer patients who underwent 4-fractionated DTT. They had 4 or 5 radiopaque markers around a lung tumor. Before beam delivery, the orthogonal x-ray fluoroscopic monitoring was done for 20-40 s. Then, 3D positions of all markers were detected on the x-ray fluoroscopic images, and a target (Pt) and three or less markers to estimate the target ware selected. First, |d| was defined as the distance from target to the geometric center of markers at end-exhalation phase on the initial day of the treatment. The |d| was constant during the treatment periods. Next, the range of respiratory motion was calculated as the root-mean-square (RMS) of the difference between respiratory positions at each phase and its baseline at and-exhalation phase for the target and the geometric center. Then, ΔRM was defined as the double of the average between them. The estimated target position (Pt') was computed by adding each geometric center to d. Three dimensional RMS of the difference between Pt and Pt' was defined as TRE. These procedures were repeatedly performed by changing the target and the combination of markers to estimate the target. Finally, the TRE map was created by convolving the raw TRE data with Cauchy distribution, to investigate the tendency of the TRE.

Results: Mean |d| was 52.3 (range, 9.5 to 126.6) mm, 46.2 (range, 6.7 to 119.1) mm, 44.5 (range, 3.3 to 106.2) mm for one-, two- and three-marker cases, respectively. Mean ΔRM was 18.4 (range, 3.3 to 46.0) mm, 18.1 (range, 3.3 to 44.5) mm, 17.5 (range, 3.4 to 44.0) mm for one-, two- and three-marker cases, respectively. Figure 1 shows that the TRE was within 4 mm for |d| of less than 20 mm. The TRE became larger interfractionally, which was derived from the displacement of the geometric center. Increasing the number of markers to estimate the Pt tended to reduce the TRE, which was remarkable for |d| greater than 40 mm.

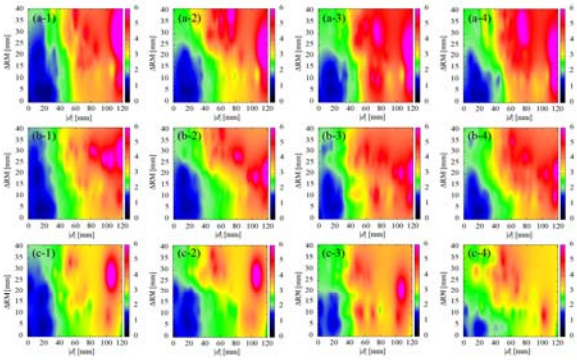

Figure 1. The TRE map created by convolving the original TRE data with Cauchy distribution. The x-axis, y-axis, and color-bar is |d|, ΔRM, and TRE, respectively. Over 6 mm TRE is depicted as magenta. (a) to (c) indicate the number of markers used to estimate the target. Top: single marker. Middle: two markers. Bottom: Three markers. (1) to (4) following (a) to (c) represent 1st fraction to 4th fraction.

Conclusions: It was found that |d| had an impact on the TRE more than ΔRM. Our study has demonstrated that it is important to place the geometric center close to the target. For fiducial-marker-based DTT, the variation in the TRE should be incorporated into treatment plans.

PD-0464

Adaptive search area template matching for image-based lung tumor tracking

P. Mercea[1], H. Teske[1], K. Giske[1], R. Bendl[2]

[1]German Cancer Research Center (DKFZ), Division of Medical Physics in Radiation Oncology, Heidelberg, Germany
[2]Heilbronn University, Faculty of Medical Informatics, Heilbronn, Germany

Purpose/Objective: Beam tracking and gating approaches rely on fast and accurate detection of intra-fractional tumor motion. Imaging of the inner anatomy allows for both, a non-invasive and at the same time direct monitoring of organ motion. When it comes to real-time imaging of the thoracic cavity, fluoroscopy is well-suited. For motion detection using such imaging, template matching has shown to be a promising approach. However, frequently changing overlaps of the tumor with dense structures in the projection images and potential baseline drifts can decrease the tracking accuracy of this method or even cause it to fail. The purpose of this work was to develop a template matching based approach for tumor tracking robust against the listed pitfalls and applicable in real-time.

Materials and Methods: The algorithm implemented in this work was evaluated on a fluoroscopic image set containing of 116 frames (25 for training; 91 for testing). Normalized cross-correlation (NCC) is used as similarity measure for matching. The correlation calculation is based on functionality provided by the open source OpenCV library. Unlike basic template matching, the search region in our developed algorithm is determined and adapted iteratively. Starting from the position detected in the previous frame and with a template-sized search area, matching and enlargement of the search area are performed alternately. In case that the highest correlation coefficient is found for the same position in subsequent enlargement steps this position is taken as the tracking result. Due to this approach, baseline drifts can be compensated for. Moreover, the algorithm supports the use of multiple templates in order to improve robustness against recurring tumor overlaps with dense structures. Due to